Activity-based protein profiling in drug-discovery

Esbroeck, A.C.M. van

2

Activity-based protein profiling of the human ischemic heart

A.C.M. van Esbroeck
Z.V. Varga
X. Di
E.J. van Rooden
V.E. Toth
Z. Onodi
P. Leszek
M. Kuśmierczyk
P. Ferdinandy
T. Hankemeier
M. van der Stelt
P. Pacher

ABSTRACT | Acute myocardial infarction and subsequent post-infarction heart failure are among the leading causes of mortality worldwide. Recently, the endocannabinoid system (ECS) has emerged as a critical modulator of cardiovascular disease, but the role of endocannabinoid metabolic enzymes had not been investigated thus far. Here, targeted lipidomics and activity-based protein profiling (ABPP) enabled investigation of the endocannabinoids and their metabolic enzymes in ischemic end-stage failing human hearts and non-failing controls. Based on lipidomics analysis, two subgroups were identified within the ischemic group; the first similar to control hearts and the second with decreased levels of the endocannabinoid 2-arachidonoyl-glycerol (2-AG) and drastically increased levels of the endocannabinoid anandamide (AEA), other *N*-acylethanolamines (NAEs) and free fatty acids. The altered lipid profile was accompanied by strong reductions in the activity of 13 hydrolases, including the 2-AG hydrolytic enzyme monoacylglycerol lipase (MGLL). These data suggest the presence of different biological states within the ischemic group, despite the lack of a clinical characteristic clearly distinguishing the patients. In addition, this study demonstrates ABPP as a tool to rapidly analyze enzyme activity in clinical samples, which may be valuable for drug-target and biomarker discovery.

Manuscript in preparation

Introduction

Ischemic heart disease, involving acute myocardial infarction and subsequent heart failure development, was responsible for 12.7% of the total global mortality (2008), thereby making it the leading cause of mortality worldwide[1]. Recently, the endocannabinoid system (ECS) has emerged as a modulator of the cardiovascular system, especially under diseased conditions[2–4]. The ECS is comprised of the cannabinoid receptor type 1 and 2 (CB1R, CB2R), their endogenous ligands, the endocannabinoids 2-arachidonoylglycerol (2-AG) and anandamide (AEA), and their metabolic enzymes (Figure 1)[5]. Diacylglycerol lipase α and β (DAGLα, DAGLβ) are the two main 2-AG biosynthetic enzymes[6]. The majority of 2-AG is hydrolyzed to arachidonic acid (AA) by monoacylglycerol lipase (MGLL)[7,8], but α,β-hydrolase domain containing proteins 6 and 12 (ABHD6, ABHD12) hydrolyze 2-AG as well[8–10]. The existence of multiple *N*-acylethanolamine (NAE) metabolic pathways makes AEA biosynthesis more complex. Direct hydrolysis of *N*-acylphospatidylethanolamines (NAPEs) to NAEs by NAPE phosholipase D (NAPE-PLD), is considered the canonical pathway[11], but alternative multi-step pathways exist as well[11]. The NAEs are hydrolyzed to ethanolamines and free fatty acids by fatty acid amide hydrolase (FAAH)[12,13]. Of note, several other NAE species have been reported as bioactive lipids, suggesting an important modulatory role for this lipid class. For example, oleoylethanolamide (OEA) and stearoylethanolamide (SEA) have anorexic effects in the periphery[14,15] and palmitoylethanolamide (PEA) was reported to enhance antinociception[16,17].

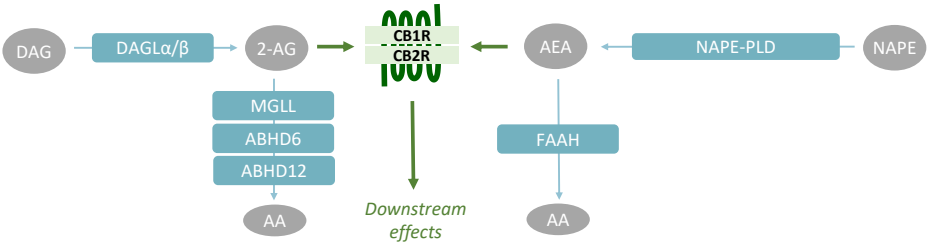

Figure 1 | The endocanabinoid system. The endocannabinoid system comprises of cannabinoid receptors type 1 and 2 (CB1R, CB2R), their endogenous ligands 2-arachidonoylglycerol (2-AG) and anandamide (AEA) and their metabolic enzymes: diacylglycerol lipase α and β (DAGLα, DAGLβ), monoacylglycerol lipase (MGLL), α,β-hydrolase domain containing proteins 6 and 12 (ABHD6, ABHD12), *N*-acylphosphatidylethanolamine phospholipase D (NAPE-PLD), and fatty acid amide hydrolase (FAAH). Alternative multi-step pathways for AEA biosynthesis are not shown.

The ECS regulates a broad spectrum of physiological and pathological processes, including energy balance, obesity, pain, inflammation, neurological and immunological disorders[18–20]. In the cardiovascular system, the endocannabinoids are implicated in various contexts in receptor dependent and independent cardiac and vascular effects, including vasodilation and vasoconstriction, cardiac protection against atherogenic inflammation, depression of cardiac function, and cell death of cardiomyocytes and endothelial cells[3,21–23]. *In vivo* cardiovascular effects of the endocannabinoids may be exerted through the central and peripheral nervous system as well as through direct

effects on the myocardium and vasculature[24,25]. The two cannabinoid receptors have been shown to have opposing effects, e.g. CB1R facilitates the development of cardiometabolic disease and cardiac dysfunction[3,26], whereas CB2R mainly exerts anti-inflammatory effects[3,27,28].

CB1R-mediated endocannabinoid signaling has been implicated in the pathogenesis of shock, atherosclerosis, and numerous forms of cardiomyopathies (ischemic, diabetic, doxorubicin-induced)[3,20]. The beneficial *in vivo* effects of CB2R agonists in rodent models of myocardial infarction have primarily been attributed to limiting inflammatory cell infiltration[27]. FAAH knockout mice, having a threefold increase in myocardial AEA, displayed increased mortality, myocardial injury and neutrophil infiltration in experimental models of cardiomyopathy in a CB1R-dependent manner[29] and FAAH deficiency also enhanced intra-plaque neutrophil recruitment in atherosclerotic mice[30]. In obese humans, increased plasma levels of AEA and 2-AG strongly correlated with impaired coronary endothelial function and adverse cardiovascular events[31,32]. In epicardial fat from ischemic human hearts, CB1R was upregulated, accompanied by down-regulation of CB2R and FAAH[33]. Similar upregulation of CB1R was observed in atherosclerotic coronary artery sections from patients with unstable angina and in obese human subjects[34]. In the Chinese Han population, a G1359A polymorphism in the CB1R gene was also linked to coronary artery disease[35]. These findings strongly suggest that the primary cardiovascular effects of endocannabinoids are deleterious and CB1R-mediated. Nonetheless, endocannabinoids have also been shown to exert protective effects in the heart via CB1R/CB2R-independent mechanisms, mostly based on *ex vivo* and indirect studies[27].

Despite extensive investigation on the endocannabinoids and their receptors in cardiac (dys)function, only little is known about the endocannabinoid metabolic enzymes. Most endocannabinoid metabolic enzymes, with the exception of NAPE-PLD, belong to the serine hydrolase family. This protein class can be targeted by activity-based probes covalently interacting with their catalytic serine residue. Activity-based probes are used in chemical proteomics to assess the functional state of an entire enzyme classes in complex biological samples[36–38]. In this study, the endocannabinoid metabolic enzymes were evaluated in ischemic end-stage failing human hearts and non-failing controls by chemical proteomics.

Results & Discussion

To investigate the involvement of the ECS in cardiac ischemia, tissue from the left ventricle was obtained from patients with terminal-stage heart failure (due to previous ischemic pathology) indicated for heart transplantation, as well as from non-failing control hearts (n=6, Table 1). The expression levels of ECS-related proteins in control and ischemic failing hearts were determined by quantitative real-time polymerase chain reaction (qRT-PCR) (Figure 2). CB1R (*CNR1*) expression strongly increased in half of the ischemic samples, however the overall increase was not significant (p=0.08). Reduced expression of the 2-AG biosynthetic enzyme DAGLβ and the 2-AG hydrolytic enzymes MGLL and ABHD6 was observed in the ischemic tissue. The AEA metabolic enzymes were not significantly altered, nor was CB2R (*CNR2*) expression.

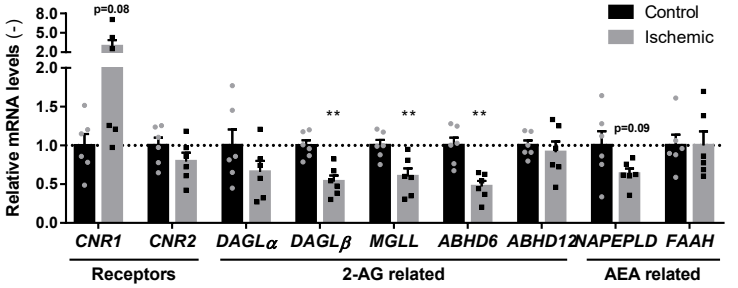

Figure 2 | Quantitative PCR on ECS-related genes in cardiac ischemia. mRNA levels of endocannabinoid related genes were normalized to house-keeping gene hypoxanthine-guanine phosphoribosyltransferase (*HPRT*) expression and expressed relative to control (mean ± SEM, two-tailed *t*-test: ** $p < 0.01$).

In light of the altered mRNA expression of ECS-related enzymes, the endocannabinoid levels in control and ischemic failing cardiac tissues were compared. Lipids were extracted from a second set of cardiac tissues (n=9, Table 1) and were analyzed by liquid chromatography coupled to mass spectrometry (LC-MS) (Figure 3, Supplementary Figure S1A). NAEs, free fatty acids (FFA) and cortisol (COR) were included in the assay. The NAEs and their related FFA levels had strongly increased in the ischemic failing tissues (Figure 3, Supplementary Figure S1B). However, based on their lipid profile, the ischemic samples could be categorized into two separate subgroups. The first (Ischemic 1: I1-I3, I8-I9) had a lipid profile similar to control for most lipids including the endocannabinoids. Only several lipids were increased, including *N*-docosahexaenoylethanolamide (DHEA), eicosapentaenoyl-ethanolamide (EPEA), α- and γ- linoleic acid (α-LA and γ-LA) (maximum fold-change: 2.8). In contrast, all NAE and FFA levels were increased with a fold change ranging from 4 to 120 in the second subgroup (Ischemic 2: I4-I7) as compared to controls. In addition, the endocannabinoid AEA was increased by a 31 ± 13-fold, while 2-AG was significantly reduced by a 5-fold in this subgroup.

Table 1 | Clinical characteristics of study populations. Values are given as mean ± SEM. Set A: Figure 2. Set B: Figures 3-5. NYHA: New York Heart Association (3.5 is included in class IV), LVED: left ventricular end-diastolic diameter, LVSD: left ventricular end-systolic diameter, PW: posterior wall-thickness, IVS: interventricular septum thickness; SVR: systemic vascular resistance, CO: cardiac output, BMI: body mass index, n.a.: not applicable. Subgroups Ischemic 1 and 2 (set B) were compared by two-tailed *t*-test: * $p < 0.05$ *** $p < 0.001$.

	Control Set A	Ischemic Set A	Control Set B H1-9	Ischemic Set B I1-9	Ischemic 1 Set B I1-3, 8-9	Ischemic 2 Set B I4-7
Samples (n)	6	6	9	9	5	4
Gender (female/male)	1 / 5	1 / 5	2 / 7	9	5	4
Age (year)	34.7 ± 4.5	56.2 ± 4.1	37.8 ± 3.8	58.0 ± 2.7	60.4 ± 2.5	55.0 ± 5.5
BMI (kg/m^2)	26.0 ± 5.0	26.1 ± 2.3	25.2 ± 1.3	26.6 ± 1.1	28.7 ± 1.2	24.0 ± 1.0 *
NYHA functional class I/II/III/IV (n)	n.a.	0/1/2/3	n.a.	0/1/5/3	0/1/2/2	0/0/3/1
CO (L/min)	n.a.	3.9 ± 0.6	n.a.	4.0 ± 0.21	4.5 ± 0.1	3.4 ± 0.2 ***
LVED (mm)	n.a.	69.2 ± 2.5	n.a.	75.0 ± 3.2	70.2 ± 3.6	81.0 ± 4.4
LVSD (mm)	n.a.	63.0 ± 3.2	n.a.	67.8 ± 4.5	62.3 ± 6.7	73.3 ± 5.5
PW (mm)	n.a.	9.1 ± 0.7	n.a.	8.4 ± 0.8	9.8 ± 1.0	6.7 ± 0.5 *
IVS (mm)	n.a.	8.4 ± 1.1	n.a.	9.5 ± 0.7	10.2 ± 1.2	8.7 ± 0.6
SVR (mmHg·min/L)	n.a.	18.3 ± 1.8	n.a.	19.0 ± 2.2	15.1 ± 2.5	23.8 ± 2.2 *

Increased AEA levels have been reported in the past e.g. due to various forms of ischemia/reperfusion (I/R) (e.g. hepatic, brain). In the liver, I/R increased 2-AG and AEA levels positively correlated with tissue damage markers such as tumor necrosis factor α (TNF-α), but inflammatory stimuli *per se* only increased AEA levels[39]. NAE levels have also been shown to drastically increase post-mortem[40] and in infarcted myocardium[41-44], thus suggesting the observed effects may be related to the extent of tissue injury. Of note, there were no obvious differences in clinical characteristics (gender, age, co-morbidity, recent ischemic events, etc.) between the two ischemic subgroups. Nonetheless, cardiac function in the second subgroup was more severely affected based on significantly decreased cardiac output (CO) and increased systemic vascular resistance (SVR) (Table 2). In addition, the body mass index (BMI) of the second subgroup was significantly lower than that of the first subgroup; however, it was not significantly different from controls.

Next, the activity of the ECS metabolic enzymes was investigated by activity-based protein profiling (ABPP). The tissue was lysed by dounce homogenization and clear lysates were labeled with fluorescent activity-based probes (Figure 4), which enabled visualization of probe targets by sodium dodecyl sulfate polyacrylamide gel electrophoresis (SDS-PAGE) and in-gel fluorescence scanning. FP-TAMRA, a broad spectrum serine hydrolase probe fluorophosphonate-rhodamine (FP-TAMRA), labels ABHD6, MGLL, and FAAH amongst many other hydrolases[36,38]. The tailored lipase probe MB064 preferentially reacts with the DAGLα, DAGLβ, ABHD6, and ABHD12[37,45]. Probes DH379[46] and DH463 enabled more selective the labeling of DAGL/ABHD6 and MGLL respectively.

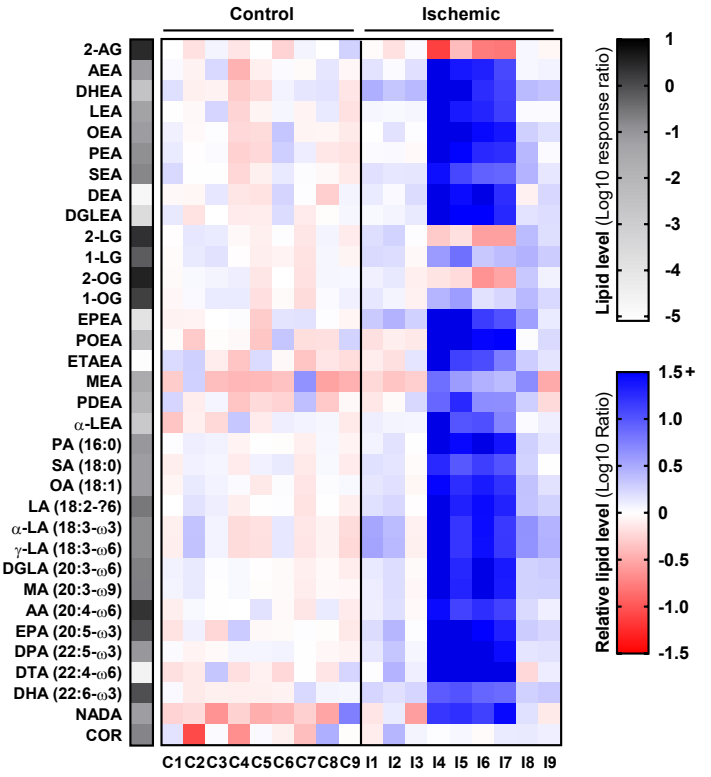

Figure 3 | Ischemic heart tissues can be categorized into subgroups based on divergent lipid profiles. Heatmap summary of lipid analysis of healthy (control) and ischemic cardiac tissue. Lipid levels were normalized to tissue weight and are expressed as mean response ratio of controls (grayscale, log10) or relative to mean control (red-blue scale, log10 ratio). Detailed lipid characteristics in Table 3.

In total, more than 20 hydrolases were labeled, including MGLL (33 and 35 kDa) (Figure 4). The overall hydrolase activity in ischemic samples I4-I7 (*, subgroup 2 based on lipid profile) was reduced as compared to the remaining ischemic samples and controls for which only limited deviations in labeling were observed. In addition, MGLL activity and expression were nearly abolished in I4-7 (Figure 4B, D, F). However, there were no obvious differences in the overall protein staining (Figure 4E) and general post-mortem degradation by autolysis thus appears unlikely. Interestingly, an additional band was observed in the activity profile of samples I4-I7 (Figure 4B, indicated with #). Of note, the other ECS metabolic hydrolases, including DAGLα (~120 kDa), DAGLβ (~70 kDa), ABHD6 (~35 kDa), and FAAH (~60 kDa) were not detected (Figure 4A, C), even though ABHD6 activity was detected in murine myocardium in the past[47].

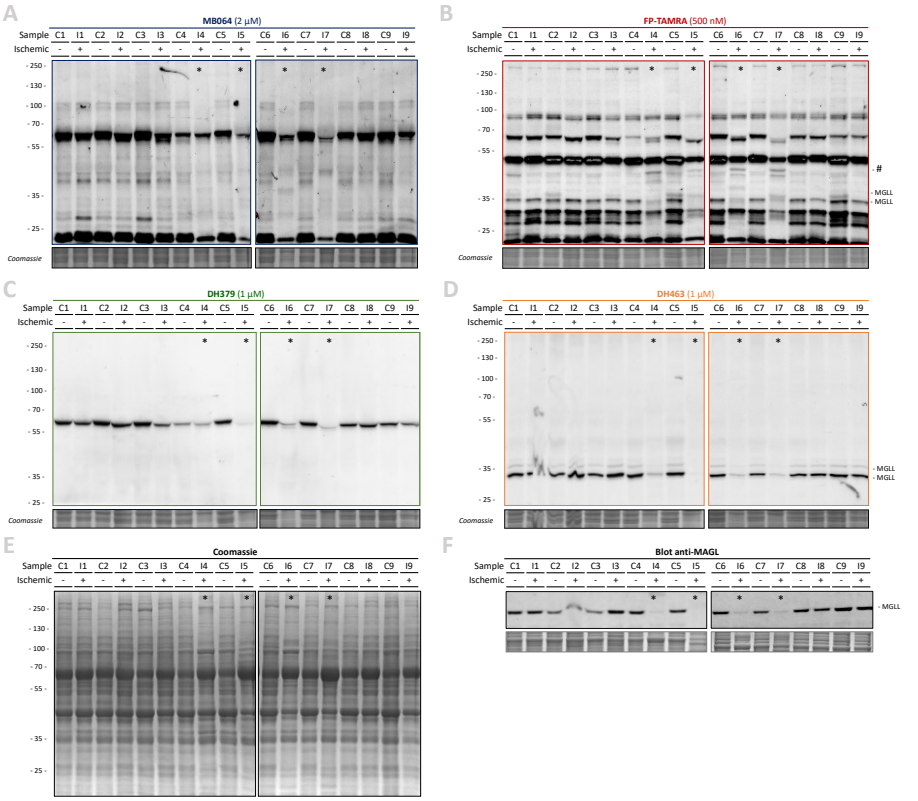

Figure 4 | Activity-based protein profiling of healthy and ischemic human hearts. (**A**-**D**) Gel-based ABPP analysis of healthy (control) and ischemic cardiac tissue. Whole lysates were labeled with activity-based probes (20 min, rt), resolved by SDS-PAGE and in-gel fluorescence was detected. Coomassie served as a protein loading control. (**A**) β-lactone probe MB064 (2 µM). (**B**) Broad-spectrum hydrolase probe FP-TAMRA (500 nM). (**C**) DAGL-probe DH379 (1 µM). (**D**) MAGL-probe DH459 (1 µM). (**E**) Coomassie staining. (**F**) Western-blot using anti-MGLL (1:200, O/N, 4 °C) verified MGLL expression. * Denotes samples with overall reduced serine hydrolase labeling.

The biotinylated counterparts of FP-TAMRA and MB064, FP-biotin and MB108 respectively, were then used for target identification by mass spectrometry-based chemical proteomics (Figure 5). In total, 31 hydrolases were identified, including MGLL as the only ECS-related hydrolase (Figure 5A, Supplementary Table S1). A slight, but non-significant, upregulation of CES1, NCEH1, and DPP4 was observed in the ischemic group, as well as downregulation of several hydrolases, including MGLL (Figure 5B). Strikingly, separation of the ischemic samples into two subgroups (based on lipid profile, Figure 3) revealed that 13 hydrolase activities, including MGLL, were drastically and significantly reduced in the subgroup with an altered lipid profile (Ischemic 2, Figure 5C). Hydrolase activities from the first subgroup, however, were not significantly altered. Notably, not all hydrolase activities were affected in the second subgroup and the extent of activity reduction is different between the altered hydrolases. This reinforces the hypothesis that the observed alterations in these samples are indeed not artefacts resulting from a general process such as post-mortem autolysis.

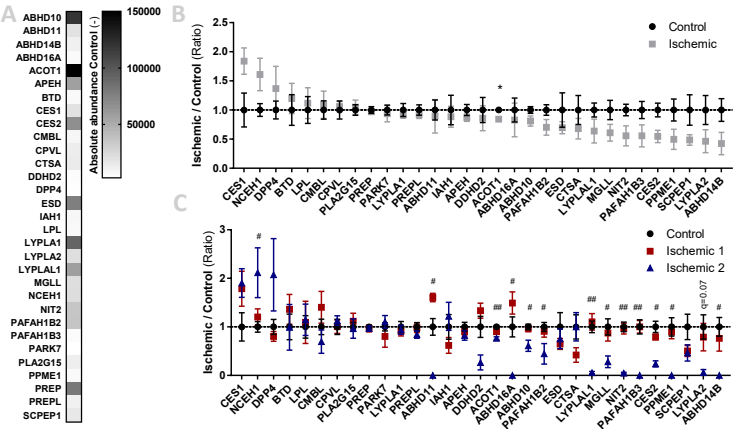

Figure 5 | Activity-based proteomics on healthy and ischemic heart tissues. (**A**-**C**) Lysates from healthy (control) and ischemic cardiac tissues were labeled with MB108 and FP-biotin (10 µM each, 30 min, 37 °C) and analyzed by mass-spectrometry. A pre-boiled sample (10% SDS, 100 °C, 5 min) served as negative control. (**A**) Heatmap summary of mean abundance of hydrolases from control tissues. (**B**) Hydrolase activity relative to mean control. Data is expressed as mean ± SEM (n=9), *t*-test with Benjamini-Hochberg correction: * q < 0.05. (**C**) Hydrolase activity relative to mean control, ischemic samples categorized in subgroups. Data is expressed as mean ± SEM (control n=9, ischemic 1 n=5, ischemic 2 n=4), *t*-test with Benjamini-Hochberg correction. Control versus ischemic 1: not significant; control versus ischemic 2: # q < 0.05, ## q < 0.01.

Taken together, lipidomics and ABPP enabled the identification of a subgroup within the ischemic sample set, which showed drastic increases in NAE and FFA levels, whereas many hydrolase activities had decreased. Aside from MGLL, no endocannabinoid metabolic enzymes were detected, possibly due to instability or inactivity as a result of tissue preparation. Despite accurate sample handling, differences in the sample collection procedure cannot be excluded as a potential cause for the observed subgroups. In addition, therapeutic interventions or unknown clinical factors may separate the ischemic tissues from one another. Nonetheless these data demonstrated that ABPP can be used for the rapid analysis of serine hydrolases in clinical samples. In the future, this technique may aid in the discovery of drug targets or biomarkers.

Conclusion

In summary, an MS-based approach was used to investigate the endocannabinoids and their metabolic enzymes in cardiac ischemia using ischemic end-stage failing hearts and non-failing controls. Targeted lipidomics analysis revealed the existence of two subgroups within the ischemic samples; the first largely similar to controls and the second with decreased 2-AG and increased AEA, NAE and FFA levels. The altered lipid profile was accompanied by a strong reduction in the activity of multiple hydrolases, including the 2-AG hydrolytic enzyme MGLL. These data suggested the presence of different biological states within the ischemic group, possibly the extent of tissue injury, despite the lack of a clinical characteristic separating the patients other than cardiac damage. In addition, this study demonstrated ABPP as a tool to rapidly assess clinical samples which may be valuable in drug-target and biomarker discovery.

Experimental procedures

Materials and probes

Activity-based fluorophosphonate-based probes FP-TAMRA and FP-biotin were purchased from ThermoFisher and Santa Cruz biotechnology respectively. MB064 and MB108 were synthesized in-house as previously described[45]. All synthesized compounds were at least 95% pure and were analyzed by LC-MS, NMR and HRMS. Other chemicals, reagents, and primers were purchased from Sigma Aldrich unless indicated otherwise.

Ethical statement

All experimental procedures were done in accordance with the ethical standards of the responsible institutional and national committee on human experimentation, adhering to the Helsinki Declaration (1975). Written informed consent was obtained from all patients involved in the study according to the protocol approved by the Local Ethics Committees of the Institute of Cardiology, Warszawa, Poland (IK-NP-0021-24/1426/14).

Sample collection and preparation

Healthy (control) human hearts were obtained from organ donor patients (n=6/9) whose hearts were not used for transplantation due to technical reasons (e.g. donor/recipient incompatibility). The donors did not have any relevant previous cardiological history or any abnormalities in ECG and echocardiography (left ventricle dimensions/contractility within normal ranges). Explanted failing hearts were obtained from patients suffering from end-stage advanced heart failure of ischemic etiology (n=6/9).

Sample collection was performed as previously described[48]. In brief, human tissue samples were taken at the time of heart explanation (avoiding scarred, fibrotic, or adipose tissue, endocardium, epicardium, or coronary vessels). The samples were rinsed immediately in saline, blotted dry, frozen in liquid nitrogen, powdered with a pestle and mortar in liquid nitrogen and stored in cryovials at -80 °C until further analysis.

Quantitative real-time PCR

RNA isolation

Total RNA was isolated from left ventricular samples (n = 6) with a chloroform/isopropanol precipitation method. In brief, Qiazol® (Qiagen) was added to each sample and homogenized with TissueLyser (Qiagen). Homogenates were centrifuged and DNA and protein were precipitated from the clean upper phase with chloroform. Total RNA was precipitated with isopropanol and pellets were washed twice with ethanol (VWR). Finally, total RNA was resuspended in nuclease-free water, and RNA concentration was determined by spectrophotometry (NanoDrop, Thermo Fischer Scientific).

cDNA synthesis

cDNA was synthesized from 1 µg total RNA by Sensifast cDNA synthesis kit (Bioline) according to the manufacturers protocol. cDNA was diluted 20 times with RNAse-free water. qRT-PCR reactions were performed on a LightCycler® 480 II instrument (Roche) by using SensiFAST SYBR Green master mix (Bioline). Polymerase was heat-activated for 2 min at 95 °C and targets were amplified and quantified in 40 cycles (denaturation: 5 s at 93 °C; annealing: 10 s at 60 °C; synthesis: 20 s at 72 °C). Forward and reverse primers for the fatty acid amide hydrolase (*FAAH*), cannabinoid receptor 1 (*CNR1*), cannabinoid receptor 2 (*CNR2*), diacylglycerol lipase α (*DAGLα*), diacylglycerol lipase β (*DAGLβ*), monoacylglycerol lipase (*MGLL*), *N*-acylphosphatidylethanolamine

phospholipase D (*NAPEPLD*), α/β-hydrolase domain-containing 6 (*ABHD6*), α/β-hydrolase domain-containing 12 (*Abhd12*) were used for analysis. Hypoxanthine-guanine phosphoribosyltransferase (*HPRT*) was used as a housekeeping gene. Results were calculated with $2^{-\Delta\Delta C_P}$ evaluation method. Primer sequences are shown in Table 2.

Table 2 | qPCR primers.

Gene	Accession number	Product (bp)	Primer	Primer Sequence
CNR1	NM_016083.5	363	Forward	CCTTTTGCTGCCTAAATCCAC
			Reverse	CCACTGCTCAAACATCTGAC
CNR2	NM_001841.3	71	Forward	CCTTTTGCTGCCTAAATCCAC
			Reverse	AACAACTGGGACTCCTCAGC
DAGLA	NM_006133.3	130	Forward	TGCTCTTCGGCCTGGTCTAT
			Reverse	CGCATGCTCAGCCAGATGAT
DAGLB	NM_139179.4	161	Forward	GAGTGCTGTGGTGGATTGGC
			Reverse	TCTCATGCTGACACACATGA
MGLL	NM_007283.6	162	Forward	CAAGGCCCTCATCTTTGTGT
			Reverse	ACGTGGAAGTCAGACACTAC
ABHD6	NM_001320126.1	86	Forward	AGACATGTTGGCCAAGTCAA
			Reverse	TCCTGGGTCTTTCCATCACT
ABHD12	NM_001042472.2	232	Forward	TATTGGAGTCTGGCACAC
			Reverse	TGTTCCTACTGAGTCACC
NAPEPLD	NM_001122838.1	178	Forward	GAAGCTGGCTTAAGAGTCAC
			Reverse	CCGCATCTATTGGAGGGAGT
FAAH	NM_000194.3	66	Forward	GCCTCAAGGAATGCTTCAGC
			Reverse	TGCCCTCATTCAGGCTCAAG
HRPT	NM_001441.2	192	Forward	TGCTCGAGATGTGATGAAGG
			Reverse	TCCCCTGTTGACTGGTCATT

Targeted lipidomics

Lipid extraction

Lipid extraction was performed as previously described[49], with minor adaptations. In brief, ~50 mg tissue was weighed into a pre-cooled 1.5 mL Eppendorf tube and reconstituted in ice-cold ammonium acetate buffer (0.1 M, pH 4) (4 µL/mg tissue). The tissue was finely cut using chirurgical scissors and subsequently homogenized by probe sonication (3 cycles, 10 s, 30% amplitude) while kept on ice. Samples were spiked with 10 µL of deuterated internal standard mix (Table 1). After extraction with 1000 µL methyl *tert*-butyl ether (MTBE), the tubes were thoroughly mixed for 5 min using a bullet blender (Next Advance) at medium speed, followed by a centrifugation step (16,000 *g*, 5 min, 4 °C). Next, 850 µL of the upper MTBE layer was transferred to clean 1.5 mL Eppendorf tube. Samples were dried in a speedvac (Eppendorf) followed by reconstitution in acetonitrile:water (50 µL, 90:10, v/v). The reconstituted samples were centrifuged (16,000 *g*, 5 min, 4 °C) before transferring into LC-MS vials. 5 µL of each sample was injected into the LC-MS/MS system.

LC-MS/MS analysis

LC-MS/MS analysis was performed as previously described[49], with minor adaptations. A targeted analysis of 31 compounds, including endocannabinoids and related *N*-acylethanolamines (NAEs) along with the fatty acids (Table 2), was measured using an Acquity UPLC I class Binary solvent manager pump (Waters) in conjugation with AB SCIEX 6500 quadrupole-ion trap (AB Sciex). The separation was performed with an Acquity HSS T3 column (1.2 × 100 mm, 1.8 µm) maintained at 45 °C. The aqueous mobile phase A consisted of 2 mM ammonium formate and 10 mM formic acid, and the organic mobile phase B was acetonitrile. The flow rate was set

to 0.55 mL/min; initial gradient conditions were 55% B held for 2 min and linearly ramped to 100% B over 6 min and held for 2 min; after 10 s the system returned to initial conditions and held 2 min next injection. Electrospray ionization-MS and a selective Multiple Reaction Mode (MRM) was used for endocannabinoid quantification. Individually optimized MRM transitions using their synthetic standards for target compounds and internal standards are described in Table 3.

Table 3 | LC-MS Standards and internal standards for lipidomics analysis.

Standards				
Abbreviation	**Metabolite**	**Q1**	**Q3**	**Polarity**
1&2-AG	2&1-Arachidonoylglycerol (20:4)	379	287	+
AEA	Anandamide (20:4)	348	62	+
DHEA	*N*-docosahexaenoylethanolamide (22:6)	372	62	+
LEA	*N*-linoleoylethanolamide (18:2)	324	62	+
NADA	*N*-arachidonoyl dopamine (28:4)	440	137	+
OEA	*N*-oleoylethanolamide (18:1)	326	62	+
PEA	*N*-palmitoylethanolamide (16:0)	300	62	+
SEA	*N*-stearoylethanolamide (18:0)	328	62	+
2-AGE	2-arachidonyl glycerol ether (20:4)	365	273	+
DEA	*N*-docosatetraenoylethanolamide (22:4)	376	62	+
DGLEA	Dihomo-γ-linolenoylethanolamide (18:3)	350	62	+
O-AEA	*O*-arachidonoyleethanolamine (20:4)	348	62	+
2-LG	2-Linoleoyl glycerol (18:2)	355	263	+
1-LG	1-Linoleoyl glycerol (18:2)	355	263	+
2-OG	2-Oleoyl glycerol (18:1)	357	265	+
EPEA	Eicosapentaenoyl ethanolamide (20:5)	346	62	+
POEA	*N*-palmitoleoylethanolamide (16:1)	298	62	+
ETAEA	Eicosatrienoic acid ethanolamide (20:3)	350	62	+
PDEA	*N*-pentadecanoylethanolamide (15:0)	286	62	+
α-LEA	*N*-α-linolenylethanolamide (18:2)	322	62	+
OA	Oleic acid (18:1)	281	263	-
LA	Linoleic acid (18:2-ω6)	279	261	-
α-LA	α-linolenic acid (18:3-ω3)	277	233	-
γ-LA	γ-linolenic acid (18:3-ω6)	277	233	-
DGLA	Dihomo-γ-linolenic acid (20:3-ω6)	305	261	-
MA	Mead acid (20:3-ω9)	305	261	-
AA	Arachidonic acid (20:4-ω6)	303	259	-
EPA	Eicosapentaenoic acid (20:5-ω3)	301	257	-
DTA	Docosatetraenoic acid (22:4-ω6)	332	288	-
DHA	Docosahexaenoic acid (22:6-ω3)	327	283	-
Internal Standards				
Abbreviation	**Metabolite**	**Q1**	**Q3**	**Polarity**
2-AG (20:4)-d8	2-Arachidonoylglycerol-d8	387	294	+
PEA (16:0)-d4	Palmitoyl ethanolamide-d4	304	62	+
SEA (18:0)-d3	Stearoyl ethanolamide-d3	331	62	+
OEA (18:1)-d4	Oleoyl ethanolamide-d4	330	66	+
LEA (18:2)-d4	Linoleoyl ethanolamide-d4	328	66	+
AEA (20:4)-d8	Arachidonoyl ethanolamide-d8	356	62	+
DHEA (22:6)-d4	Docosahexaenoyl ethanolamide-d4	376	66	+
NADA (28:4)-d8	*N*-Arachidonoyl dopamine-d8	448	137	+

Activity-based protein profiling

Sample preparation

Cardiac tissue was dounce homogenized in ice-cold lysis buffer (250 mM sucrose, 20 mM HEPES pH 7.2, 2 mM DTT, 1 mM $MgCl_2$, 2 U/mL benzonase) and incubated on ice (15 min). Clear lysate was obtained as the supernatant fraction after two low-speed centrifugation steps (2500 *g,* 5 min, 4 °C). After dilution to 2 mg/mL in storage buffer (20 mM HEPES pH 7.2, 2 mM DTT), samples were used or flash frozen in liquid nitrogen and stored at -80 °C until further use.

Gel-based ABPP

Clear lysates (2 mg/mL) were incubated with activity-based probes MB064 (2 µM), FP-TAMRA (500 nM), DH379 (1 µM) or DH463 (1 µM) (20 min, rt). The reaction was quenched with Laemmli buffer (30 min, rt) and 20 µg protein was resolved by SDS-PAGE (10% acrylamide gel, ~80 min, 180 V) along with protein marker (PageRuler™ Plus, Thermo Fisher). In-gel fluorescence was measured in the Cy2, Cy3 and Cy5 channels (ChemiDoc™ MP, Bio-Rad) and gels were stained with Coomassie after scanning. Fluorescence was quantified and normalized to Coomassie staining using ImageLab™ software (Bio-Rad).

Chemical proteomics with label-free quantification

The chemical proteomics workflow was modified from a previously published protocol[50]. In short, for general profiling of the serine hydrolases the clear lysates (250 µg protein, 1 mg/mL) were incubated with serine hydrolase probe cocktail (10 µM MB108, 10 µM FP-Biotin, 30 min, 37 ˚C, 300 rpm). A denatured protein sample (1% SDS, 5 min, 100 ˚C) was taken along as a negative control. Precipitation, alkylation, avidin enrichment, on-bead digestion and sample preparation was performed according to protocol. Dried peptides were stored at -20 °C until LC-MS analysis. Prior to measurement, samples were reconstituted in 50 µL LC-MS solution and transferred to LC-MS vials. LC-MS data was analyzed by ProteinLynx Global SERVER™ (PLGS, Waters) and IsoQuant software[51] (www.proteomeumb.org/MZw.html) minimal peptide score 6, false discovery rate 1%). Excel was used for further analysis, with the following cut-offs: false discovery rate 1%, unique peptides ≥ 1, identified peptides ≥ 2, ratio positive over negative control ≥ 2, part of putative hydrolase target list. Graphs were created using GraphPad Prism 7 (GraphPad).

Western blot

Clear lysates (2 mg/mL) were denatured with Laemmli buffer (5 min, 100 ˚C) and 45 µg lysate was resolved by SDS-PAGE (10% acrylamide gel, 65 min, 200V) along with PageRuler™ Plus Protein Marker (Thermo Scientific). Proteins were transferred to 0.2 µm polyvinylidene difluoride membranes by Trans-Blot Turbo™ Transfer system (Bio-Rad). Membranes were washed with TBS (50 mM Tris, 150 mM NaCl) and blocked with 5% milk in TBS-T (50 mM Tris, 150 mM NaCl, 0.05% Tween 20) (1 h, rt). Membranes were then incubated with primary antibody rabbit-anti-MAGL (ab24701, Abcam, 1:200 in 5% milk in TBS-T, O/N, 4 °C) washed with TBS-T, incubated with secondary donkey-anti-rabbit Alexa647 (A-31573, Thermo Fisher; 1:10000 in 5% milk TBS-T, 1 h, rt), and washed with TBS-T and TBS. Fluorescence was detected on the ChemiDoc™ MP (Bio-Rad) in the Alexa647 channel, and Cy3/Cy5 channels for the protein marker.

Statistical methods

Statistical significance was determined by a Student's *t*-test (two-tailed, unpaired)(p-values) with Benjamini-Hochberg false discovery rate (FDR 10%, q-values) for lipidomics and proteomics data using GraphPad Prism 7 (GraphPad) software. Samples were compared to (mean) healthy controls and significance is indicated as * < 0.05, ** < 0.01, *** < 0.001.

Supplementary data

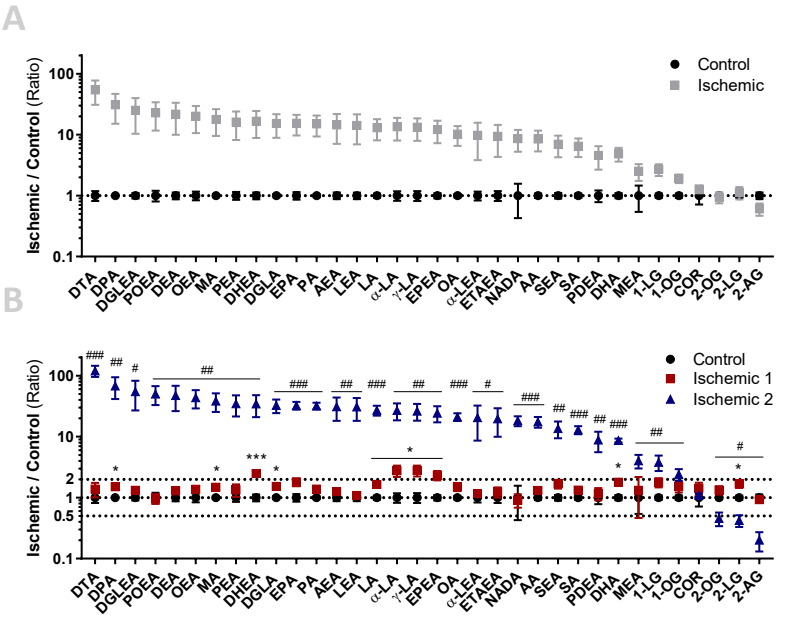

Figure S1 | Targeted lipidomics of healthy and ischemic heart tissues reveals subgroups in ischemic samples. Lipids were extracted from control and ischemic cardiac tissue, followed by targeted lipidomics analysis. Lipid levels were normalized to tissue weight and are expressed relative to mean control. (**A**) Lipid levels relative to mean control. Data is expressed as mean ± SEM (n=9), *t*-test with Benjamini-Hochberg correction for multicomparison: not significant. (**B**) Lipid levels relative to mean control, ischemic samples categorized in subgroups. Data is expressed as mean ± SEM (control: n=9, ischemic 1: n=5, ischemic 2: n=4), *t*-test with Benjamini-Hochberg correction for multicomparison. * $q < 0.05$, *** $q < 0.001$ (control vs. ischemic 1), # $q < 0.05$, ## $q < 0.01$, ### $q < 0.001$ (control vs. ischemic 2).

Table S1 | Identified hydrolase targets in human cardiac tissue. Abbreviations and descriptions as annotated on uniprot.org.

Protein	Description
ABHD10	Mycophenolic acid acyl-glucuronide esterase, mitochondrial (α,β-hydrolase domain containing protein 10)
ABHD11	Protein ABHD11 (α,β-hydrolase domain containing protein 11)
ABHD14b	Protein ABHD14b (α,β-hydrolase domain containing protein 14b)
ABHD16a	Protein ABHD16a (α,β-hydrolase domain containing protein 16a)
ACOT1	Acyl-coenzyme A thioesterase 1
APEH	Acylamino-acid-releasing enzyme (acyl-peptide hydrolase)
BTD	Biotinidase
CES1	Liver carboxylesterase 1 (carboxylesterase 1)
CES2	Cocaine esterase (carboxylesterase 2)
CMBL	Carboxymethylenebutenolidase homolog
CPVL	Probable serine carboxypeptidase CPVL (Carboxypeptidase, vitellogenic-like)
CTSA	Lysosomal protective protein (cathepsin A)
DDHD2	Phospholipase DDHD2 (DDHD domain-containing protein 2)
DPP4	Dipeptidyl peptidase 4
ESD	S-formylglutathione hydrolase
IAH1	Isoamyl acetate-hydrolyzing esterase 1 homolog
LPL	Lipoprotein lipase
LYPLA1	Acyl-protein thioesterase 1 (Lysophospholipase 1)
LYPLA2	Acyl-protein thioesterase 2 (Lysophospholipase 2)
LYPLAL1	Lysophospholipase-like protein 1
MGLL	Monoglyceride lipase (monoacylglycerol lipase)
NCEH1	Neutral cholesterol ester hydrolase 1
NIT2	Omega-amidase NIT2
PAFAH1b2	Platelet-activating factor acetylhydrolase IB subunit beta
PAFAH1b3	Platelet-activating factor acetylhydrolase IB subunit gamma
PARK7	Protein DJ-1 (Protein/nucleic acid deglycase DJ-1, parkinson disease protein 7)
PLA2G15	Group XV phospholipase A2
PPME1	Protein phosphatase methylesterase 1
PREP	Prolyl endopeptidase
PREPL	Propyl endopeptidase-like
SCPEP1	Retinoid-inducible serine carboxypeptidase (Serine carboxypeptidase 1)

References

1. Finegold, J. A., Asaria, P. & Francis, D. P. Mortality from ischaemic heart disease by country, region, and age: Statistics from World Health Organisation and United Nations. *Int. J. Cardiol.* **168,** 934–945 (2013).
2. O'Sullivan, S. E. in *Endocannabinoids* 393–422 (Springer, Cham, 2015).
3. Pacher, P., Steffens, S., Haskó, G., Schindler, T. H. & Kunos, G. *Cardiovascular effects of marijuana and synthetic cannabinoids: The good, the bad, and the ugly*. *Nature Reviews Cardiology* **15,** 151–166 (Nature Publishing Group, 2018).
4. Pacher, P. *et al.* Modulation of the endocannabinoid system in cardiovascular disease: therapeutic potential and limitations. *Hypertens.* **52,** 601–7 (2008).
5. Di Marzo, V. Endocannabinoid signaling in the brain: biosynthetic mechanisms in the limelight. *Nat. Neurosci.* **14,** 9–15 (2011).
6. Bisogno, T. *et al.* Cloning of the first sn1-DAG lipases points to the spatial and temporal regulation of endocannabinoid signaling in the brain. *J. Cell Biol.* **163,** 463–468 (2003).
7. Dinh, T. P., Freund, T. F. & Piomelli, D. A role for monoglyceride lipase in 2-arachidonoylglycerol inactivation. in *Chemistry and Physics of Lipids* **121,** 149–158 (2002).
8. Savinainen, J. R., Saario, S. M. & Laitinen, J. T. The serine hydrolases MAGL, ABHD6 and ABHD12 as guardians of 2-arachidonoylglycerol signalling through cannabinoid receptors. *Acta Physiologica* **204,** 267–276 (2012).
9. Marrs, W. R. *et al.* The serine hydrolase ABHD6 controls the accumulation and efficacy of 2-AG at cannabinoid receptors. *Nat. Neurosci.* **13,** 951–7 (2010).
10. Blankman, J. L., Simon, G. M. & Cravatt, B. F. A comprehensive profile of brain enzymes that hydrolyze the endocannabinoid 2-arachidonoylglycerol. *Chem. Biol.* **14,** 1347–1356 (2007).
11. Ueda, N., Tsuboi, K. & Uyama, T. Metabolism of endocannabinoids and related N-acylethanolamines: Canonical and alternative pathways. *FEBS J.* **280,** 1874–1894 (2013).
12. Cravatt, B. F. *et al.* Molecular characterization of an enzyme that degrades neuromodulatory fatty-acid amides. *Nature* **384,** 83–87 (1996).
13. Mckinney, M. K. & Cravatt, B. F. Structure and function of Fatty Acid Amide Hydrolase. *Annu. Rev. Biochem.* **74,** 411–432 (2005).
14. Rodríguez De Fonseca, F. *et al.* An anorexic lipid mediator regulated by feeding. *Nature* **414,** 209–212 (2001).
15. Terrazzino, S. *et al.* Stearoylethanolamide exerts anorexic effects in mice via downregulation of liver stearoyl-coenzyme A desaturase-1 mRNA expression. *Faseb J.* **18,** 1580–1582 (2004).
16. Calignano, A., Rana, G. La, Giuffrida, A. & Piomelli, D. Control of pain initiation by endogenous cannabinoids. *Nature* **394,** 277–281 (1998).
17. Jaggar, S. I., Hasnie, F. S., Sellaturay, S. & Rice, A. S. . The anti-hyperalgesic actions of the cannabinoid anandamide and the putative CB2 receptor agonist palmitoylethanolamide in visceral and somatic inflammatory pain. *Pain* **76,** 189–199 (1998).
18. Mechoulam, R. & Parker, L. A. The Endocannabinoid System and the Brain. *Annu. Rev. Psychol.* **64,** 21–47 (2012).
19. Di Marzo, V., Bifulco, M. & De Petrocellis, L. The endocannabinoid system and its therapeutic exploitation. *Nature Reviews Drug Discovery* **3,** 771–784 (2004).
20. Pacher, P., Bátkai, S. & Kunos, G. The Endocannabinoid System as an Emerging Target of Pharmacotherapy. *Pharmacol. Rev.* **58,** 389–462 (2006).
21. Hiley, C. R. Endocannabinoids and the heart. *Journal of Cardiovascular Pharmacology* **53,** 267–276 (2009).
22. Montecucco, F. & Di Marzo, V. At the heart of the matter: The endocannabinoid system in cardiovascular function and dysfunction. *Trends in Pharmacological Sciences* **33,** 331–340 (2012).

23. Pacher, P. & Kunos, G. Modulating the endocannabinoid system in human health and disease - successes and failures. *FEBS J.* **280,** 1918–1943 (2013).
24. Bátkai, S. & Pacher, P. Endocannabinoids and cardiac contractile function: Pathophysiological implications. *Pharmacological Research* **60,** 99–106 (2009).
25. Pacher, P., Bátkai, S. & Kunos, G. Cardiovascular pharmacology of cannabinoids. *Handb. Exp. Pharmacol.* 599–625 (2005).
26. Valenta, I. *et al.* Feasibility Evaluation of Myocardial Cannabinoid Type 1 Receptor Imaging in Obesity: A Translational Approach. *JACC Cardiovasc. Imaging* **11,** 320–332 (2018).
27. Steffens, S. & Pacher, P. Targeting cannabinoid receptor CB2 in cardiovascular disorders: promises and controversies. *Br. J. Pharmacol.* **167,** 313–323 (2012).
28. Pacher, P. & Mechoulam, R. *Is lipid signaling through cannabinoid 2 receptors part of a protective system? Progress in Lipid Research* **50,** 193–211 (NIH Public Access, 2011).
29. Mukhopadhyay, P. *et al.* Fatty acid amide hydrolase is a key regulator of endocannabinoid-induced myocardial tissue injury. *Free Radic. Biol. Med.* **50,** 179–195 (2011).
30. Lenglet, S. *et al.* Fatty Acid Amide Hydrolase Deficiency Enhances Intraplaque Neutrophil Recruitment in Atherosclerotic Mice. *Arterioscler. Thromb. Vasc. Biol.* **33,** 215–223 (2013).
31. Quercioli, A. *et al.* Coronary Vasomotor Control in Obesity and Morbid Obesity. *JACC Cardiovasc. Imaging* **5,** 805–815 (2012).
32. Quercioli, A. *et al.* Elevated endocannabinoid plasma levels are associated with coronary circulatory dysfunction in obesity. *Eur. Heart J.* **32,** 1369–1378 (2011).
33. Cappellano, G. *et al.* Different Expression and Function of the Endocannabinoid System in Human Epicardial Adipose Tissue in Relation to Heart Disease. *Can. J. Cardiol.* **29,** 499–509 (2013).
34. Sugamura, K. *et al.* Activated Endocannabinoid System in Coronary Artery Disease and Antiinflammatory Effects of Cannabinoid 1 Receptor Blockade on Macrophages. *Circulation* **119,** 28–36 (2009).
35. Liu, R. & Zhang, Y. G1359A polymorphism in the cannabinoid receptor-1 gene is associated with coronary artery disease in the Chinese Han population. *Clin. Lab.* **57,** 689–93 (2011).
36. Niphakis, M. J. & Cravatt, B. F. Enzyme Inhibitor Discovery by Activity-Based Protein Profiling. *Annu. Rev. Biochem.* **83,** 341–377 (2014).
37. Baggelaar, M. P. *et al.* Highly Selective, Reversible Inhibitor Identified by Comparative Chemoproteomics Modulates Diacylglycerol Lipase Activity in Neurons. *J. Am. Chem. Soc.* **137,** 8851–8857 (2015).
38. Liu, Y., Patricelli, M. P. & Cravatt, B. F. Activity-based protein profiling: The serine hydrolases. *Proc. Natl. Acad. Sci.* **96,** 14694–14699 (1999).
39. Bátkai, S. *et al.* Cannabinoid-2 receptor mediates protection against hepatic ischemia/reperfusion injury. *FASEB J.* **21,** 1788–1800 (2007).
40. Schmid, P. C. *et al.* Occurrence and postmortem generation of anandamide and other long-chain *N* -acylethanolamines in mammalian brain. *FEBS Lett.* **375,** 117–120 (1995).
41. Epps, D. E., Schmid, P. C., Natarajan, V. & Schmid, H. H. O. N-Acylethanolamine accumulation in infarcted myocardium. *Biochem. Biophys. Res. Commun.* **90,** 628–33 (1979).
42. Epps, D. E., Natarajan, V., Schmid, P. C. & Schmid, H. H. O. Accumulation of N-acylethanolamine glycerophospholipids in infarcted myocardium. *Biochim. Biophys. Acta (BBA)/Lipids Lipid Metab.* **618,** 420–430 (1980).
43. Natarajan, V., Reddy, P. V., Schmid, P. C. & Schmid, H. H. O. On the biosynthesis and metabolism of N-acylethanolamine phospholipids in infarcted dog heart. *Biochim. Biophys. Acta (BBA)/Lipids Lipid Metab.* **664,** 445–448 (1981).
44. Natarajan, V., Reddy, P. V., Schmid, P. C. & Schmid, H. H. O. N-acylation of ethanolamine phospholipids in canine myocardium. *Biochim. Biophys. Acta (BBA)/Lipids Lipid Metab.* **712,** 342–355 (1982).

45. Baggelaar, M. P. *et al.* Development of an activity-based probe and in silico design reveal highly selective inhibitors for diacylglycerol lipase-α in brain. *Angew. Chemie - Int. Ed.* **52,** 12081–12085 (2013).
46. Ogasawara, D. *et al.* Rapid and profound rewiring of brain lipid signaling networks by acute diacylglycerol lipase inhibition. *Proc. Natl. Acad. Sci.* **113,** 26–33 (2016).
47. Janssen, A. P. A. *et al.* Development of a Multiplexed Activity-Based Protein Profiling Assay to Evaluate Activity of Endocannabinoid Hydrolase Inhibitors. *ACS Chem. Biol.* **13,** 2406–2413 (2018).
48. Varga, Z. V. *et al.* Alternative splicing of NOX4 in the failing human heart. *Front. Physiol.* **8,** 935 (2017).
49. Kantae, V. *et al.* Endocannabinoid tone is higher in healthy lean South Asian than white Caucasian men. *Sci. Rep.* **7,** (2017).
50. van Rooden, E. J. *et al.* Mapping in vivo target interaction profiles of covalent inhibitors using chemical proteomics with label-free quantification. *Nat. Protoc.* **13,** 752–767 (2018).
51. Liao, Z., Wan, Y., Thomas, S. N. & Yang, A. J. IsoQuant: A software tool for stable isotope labeling by amino acids in cell culture-based mass spectrometry quantitation. *Anal. Chem.* **84,** 4535–4543 (2012).